Published in final edited form as:
Arch Biochem Biophys. 2007 August 15; 464(2): 221–227. doi:10.1016/j.abb.2007.05.017.

CONFORMATIONAL DYNAMICS IN THE F/G SEGMENT OF CYP51 FROM M*ycobacterium tuberculosis* MONITORED BY FRET

Galina I. Lepesheva[a], **Matej Seliskar**[b], **Charles G. Knutson**[a], **Nina V. Stourman**[a], **Damjana Rozman**[b], and **Michael R. Waterman**[a,*]

[a] Department of Biochemistry, Vanderbilt University School of Medicine, Nashville, TN, 37232-0146, USA

[b] Centre for Functional Genomics and Bio-Chips, Institute of Biochemistry, Faculty of Medicine, University of Ljubljana, 1000, Ljubljana, Slovenia

Abstract

A cysteine was introduced into the FG-loop (P187C) of CYP51 from *Mycobacterium tuberculosis* (MT) for selective labeling with BODIPY and fluorescence energy transfer (FRET) analysis. Forster radius for the BODIPY-heme pair was calculated assuming that the distance between the heme and Cys187 in solution corresponds to that in the crystal structure of ligand free MTCYP51. Interaction of MTCYP51 with azole inhibitors ketoconazole and fluconazole or the substrate analog estriol did not influence the fluorescence, but titration with the substrate lanosterol quenched BODIPY emission, the effect being proportional to the portion of substrate-bound MTCYP51. The detected changes correspond to ~10 Å decrease in the calculated distance between BODIPY-Cys187 and the heme. The results confirm 1) functional importance of conformational motions in the MTCYP51 F/G segment and 2) applicability of FRET to monitor them in solution.

Keywords

Cytochrome P450; sterol 14α-demethylase; ligand binding; conformational changes; FRET

The cytochrome P450 superfamily currently includes more than 6,300 enzymes (http://drnelson.utmem.edu/CytochromeP450.html) oxidizing a wide variety of xenobiotics (compounds from the environment) and endogenous substrates. Even at less than 16% amino acid identity, all P450s preserve a common overall structural fold (α-helical with orthogonal bundle architecture according to CATH classification [1]) and the set of secondary structural elements that allow the superfamily to metabolize a wide variety of diverse and unrelated structures. By now it has become quite generally accepted that this enormous catalytic versatility arises from the P450 conformational flexibility [2,3]. Ligand-induced conformational changes encompassing small to large movements are seen in the X-ray structures of several bacterial and drug-metabolizing mammalian CYPs[1] (e.g. CYPs101

*Corresponding author: Michael R. Waterman, Tel.: 615-343-1373; Fax: 615-322-4349; E-mail: michael.waterman@vanderbilt.edu.

[4], 119 [5], 158A2 [6], 2B4 [7], 2C5 [8], and 2C9 [9]). Most pronounced motions are usually observed in the substrate binding regions, including B/C and F/G segments, so that the shape of the substrate binding cavity becomes adjustable to the shape of the corresponding substrate [2,10–12].

Sterol 14α-demethylase (CYP51) is a P450 found in all biological kingdoms. It is required for sterol biosynthesis and catalyzes demethylation of 5 natural sterol substrates which have very subtle structural differences [13]. In eukaryotes this P450 is localized in the endoplasmic reticulum and in prokaryotes it is a soluble protein. The high resolution structure of soluble CYP51 from *Mycobacterium tuberculosis* (MTCYP51) has been determined by X-ray crystallography [14]. Contrary to the P450s mentioned above, in the structure of MTCYP51 (ligand free [1h5z] versus inhibitor bound (4-phenylimidazole [1e9x], fluconazole [1ea1]) or the estriol (substrate analog) bound form [1×8v]) the BC and FG loop regions are superimposed very well, with the exception of the C-terminal part of the BC-loop, which is not seen in the ligand-free and estriol-bound MTCYP51; the active site volume remaining the largest amongst known P450 structures, 2,600 $Å^3$ [14]. For comparison, the calculated active site volumes of some other CYPs are: 256 and 264 $Å^3$ for cytochrome P450cin (CYP176A) and cytochrome P450cam (CYP101) [15]), 645 $Å^3$ for CYP2C5 [16], 670$Å^3$ for CYP2C9 [17], 1440 $Å^3$ for CYP2C8 [18] and 520 to 1386 $Å^3$ for CYP3A4 [19 and 20, respectively]. An assumption that the distant location of the F/G segment (~30 Å from the heme iron) may be largely preserved in the substrate-bound sterol 14α-demethylase suggested that substrate recognition sites (SRS) 2 and 3 [21] in this CYP family (or perhaps particularly in MTCYP51) might be non-functional [22]. On the other hand, site-directed mutagenesis of five amino acid residues in this region (L172, G175, P178, R194 and D195), which are highly conserved in the CYP51 family and exposed into the substrate binding cavity of MTCYP51 has shown that all of them are essential for MTCYP51 catalytic activity at the stage of the interaction with substrate. Moreover, mutation of A197 in the middle of the MTCYP51 G-helix to the helix-breaking glycine causes about one order of magnitude enzyme activation and sharp increase in the substrate bound (high-spin) portion of the P450 in the solution upon titration with lanosterol with no influence on the calculated Kd values [23]. Based on these experimental results we hypothesized that formation of the MTCYP51 complex with substrate occurs via multiple protein-sterol interactions and requires conformational changes in the location of the F/G segment in such a way that SRSs 2 and 3 approach closer to the heme.

Because MTCYP51 remains resistant to co-crystallization with its highly hydrophobic sterol substrates as well as because an X-ray structure always represents only one minimum energy conformation (which might be influenced by crystallization conditions, crystal packing etc. [11]) we used fluorescence resonance energy transfer (FRET) between a thiol-reactive fluorescent label covalently bound to a Cys-residue artificially introduced into the region of interest and the heme, which serves as non-irradiative fluorescence acceptor, as an approach to monitor conformational changes in the F/G segment of MTCYP51 in the solution. The efficiency (E) of FRET in a donor/acceptor pair depends on the spectral overlap in the donor fluorescence emission and acceptor absorption and is sensitive to the sixth power of the distance between the donor and acceptor (r), in accordance with the equation:

$$E=R_0^6/(R_0^6+r^6), \quad (1)$$

[1]**Abbreviations used:** CYP, cytochrome P450; CYP51, sterol 14α-demthylase, FRET, fluorescence resonance energy transfer, MT, *Mycobacterium tuberculosis*

where Ro is so called Förster radius, or the distance at which the energy transfer is 50% efficient (typically 10 to 100Å [25]). The FRET method has been shown to be applicable to study intermolecular complex formation, solution dynamics and large-scale conformational changes in many proteins (e.g. [26–33]), including cytochromes P450. In P450 studies it was first used to determine intramolecular distance between the heme and a fluorescent donor (FITC) attached to the N-terminal methionine of $P450_{LM2}$ [34], and later, to monitor conformational dynamics of CYP11A1 where the same fluorescence donor was selectively attached to a Lys-residue in the K-helix (close to SRS5) [35]. More recent work by Halpert and Davydov has revealed applicability of FRET to resolve multiple substrate binding sites in CYP107A1 (EryF) [36] and CYP3A4 [37].

In the present study two surface accessible internal Cys residues in the A197G mutant of MTCYP51 were mutated and a new Cys (187) was introduced into the FG-loop as a target for selective chemical modification with a thiol-reactive probe BODIPY-FL N-(2-aminoethyl)maleimide. The labeled MTCYP51 remained enzymatically active and retained its ability to interact with ligands. We observed that the efficiency of FRET in the donor-acceptor pair BODIPY-heme is not affected by the addition of azole inhibitors or the non-metabolized substrate analog estriol but increases sharply upon titration of the enzyme with the substrate lanosterol. The data suggest large-scale motion of the FG-loop toward the heme. Such motion must decrease the MTCYP51 active site volume for better correspondence to the volume of the substrate molecule.

Materials and methods

Thiol-reactive fluorescent dyes were purchased from Molecular Probes, ketoconazole and fluconazole were from ICN, while other chemicals were from Sigma. Surface accessibilities of amino acid residues were estimated from the MTCYP51 structure [1h5z] using Swiss PDB Viewer. Site-directed mutagenesis was done using QuikChange site-directed mutagenesis kit (Stratagene). MTCYP51, wild type and the mutants, were expressed, purified and functionally characterized as described previously [23,38]. Absolute and difference absorbance spectra were recorded using a Shimadzu UV-240IPC spectrophotometer. The potentials of the mutants to form intermolecular disulfide bonds were compared by 10% PAGE in the presence and in the absence of reducing equivalents (β-mercaptoethanol, DTT).

Selective chemical modification of MTCYP51

Three thiol-reactive probes: 6-iodoacetamidofluorescein (6-IAF), fluorescein-5-maleimide and BODIPY-FL N-(2-aminoethyl)maleimide were tested as potential fluorescent labels, chemical modification carried out under the conditions suggested by Molecular Probes' Handbook of Fluorescent Probes and Research Products (Invitrogen). Because it has the best fluorescent parameters including high quantum yield, stability, insensitivity to the environment, temperature, or solvent polarity, BODIPY (absorption maximum 504 nm; emission maximum 515 nm) was selected for the further work, though some data were also reproduced using 6-iodoacetamidofluorescein as another thiol-reactive label. The final modification procedure was as follows: the S-S-bonds in the MTCYP51 A197G/C37L/C442A/P187C mutant were reduced by 10 min incubation on ice with 200-molar excess of DTT. The excess of DTT was removed by gel-filtration on a Sephadex G-50 column equilibrated with freshly degassed 50 mM potassium-phosphate buffer, pH7.0. The protein was then diluted to 100 uM, and 3-fold molar excess of BODIPY-FL-N-(2-aminoethyl)maleimide was added dropwise from a 5 mM solution in dimethylformamide with stirring in the dark. The mixture was incubated for 20 min at room temperature and the conjugate was separated from the unbound dye on a Sephadex G-50 column. The degree of labeling was determined from the absolute absorption spectrum using molar extinction

coefficients of 117 mM^{-1} cm^{-1} at 417 nm for MTCYP51 and 79 mM^{-1} cm^{-1} at 504 nm for BODIPY and subtracting the heme absorbance (equal 0.07 A_{417}) from the optical density at 504 nm: $A_{BOIYPY}=A_{504}-1/10\ A_{417}$. Absence of non-covalently bound dye was proved by precipitation of the modified MTCYP51 with acidic acetone as described previously [35], the pellet was dissolved in the same buffer containing 6 M guanidine chloride, and the amount of covalently bound BODIPY determined from the absorbance at A_{504}. BODIPY-labeled apo-protein (absent heme) was prepared by the same procedure and dialyzed overnight against 50 mM potassium-phosphate buffer, pH 7.0 to remove guanidine chloride. Absence of aggregation as a result of heme removal was confirmed by HPLC on a Superdex 200 HR 10/30 column using Waters 486 absorbance detector (wavelength 280 nm).

Measurement of FRET

The fluorescence spectra of BODIPY labeled MTCYP51 were recorded in the range 500–550 nm using a fluorimeter Fluorolog-3 (Jobin Yvon Inc., Edison NJ) at an excitation wavelength setting of 490 nm and 1.5 μM final concentration of MTCYP51 (absolute absorbance). The same emission range/excitation wavelength were used in control experiments with 6-IAF-labeled MTCYP51. The ratio between the intensities of BODIPY emission in the holo-protein and apo-protein F/F_0 (equal to the ratio of quantum yields of the label in the presence and absence of acceptor, respectively, or Q/Q_0) was used to calculate the Förster radius (R_0) for the donor-acceptor pair BODIPY/heme, using equations

$$R_0^6=E \times r^6/(1-E) \tag{2}$$

and

$$E=1-Q/Q_0 \tag{3}$$

and assuming that the distance between the fluorophor and the heme in the solution (r) corresponds to the distance in the crystal structure of the ligand free MTCYP51 [1H5Z], (r_{str}=31.97Å). BODIPY emission was further monitored upon titration of MTCYP51 with ligands; the percentage of ligand bound P450 being estimated in parallel experiments from the absorbance spectra as described previously [23,38]. Decrease in the C187-heme distance in lanosterol bound MTCYP51 was calculated from the decrease in the BODIPY emission observed upon addition of lanosterol. Because this decrease was found to be in a linear proportion with the MTCYP51 high-spin form content, the final value was then obtained by linear approximation of the changes to 100% high-spin MTCYP51. The values calculated for Förster radius, efficiency of FRET and changes in the distance were further validated using PhotochemCAD software (http://www.photochemcad.com).

Results

MTCYP51 preparation for selective labeling

MTCYP51 is a relatively good subject for selective chemical modification with thiol-reactive probes because it contains only four internal cysteines. Amongst them, C394 is coordinated to the heme iron (fifth axial ligand in the P450) and thus not available for labeling; Cys 151 is buried inside the protein globule so the probability of its modification is rather low, while C37 and C442 have higher surface accessibility (16 and 18%, respectively) (Fig. 1A). Site-directed mutagenesis of C37 (C37L) and C442 (C442A mutant) does not greatly affect either P450 expression or functional properties of MTCYP51 but substitution of C151 was found to more significantly reduce expression and activity (Table 1). Of the

three C151 mutants made, only C151A was expressed as a P450 in an amount sufficient for purification and characterization.

As the site for selective labeling, Cys was introduced into the FG loop in place of P187. We have chosen P187 for this mutation because based on structural information it has the highest exposure to the surface (65%) in the region. Besides, as we have shown earlier, though conserved in the CYP51 family, in MTCYP51 this residue can be mutated to A without significant loss of ligand binding affinity [23]. Substitution of P187 to C has practically the same effect as the P187A mutation, the mutant retains 55% of the wild type protein activity and 79% of the ability to produce type 1 spectral response to substrate addition.

Combinations of these mutations were tested to choose the best final construct for fluorescent labeling. In all cases the A197G mutant of MTCYP51 was used as a template. This activating mutation causes a four-fold increase in the amplitude of the MTCYP51 spectral response to lanosterol addition, the high-spin form content reaches about 70% [23], making it possible to monitor substrate binding by absorbance spectroscopy even if the amplitude is decreased by further amino acid substitutions and labeling. Because of this correlation between the amplitude of the spectral response and CYP51 enzymatic activity [23] we calculated the percentage of substrate-bound MTCYP51 from the high-spin form content. Contrary to many P450s which exist in the equilibrium of the high- and low-spin forms regardless of the presence of substrate, MTCYP51 [23,40] (as well as the eukaryotic CYP51 orthologs the authors are familiar with [13,38,39]) and never show any alterations in the spin-state as a result of changes in the environment (such as temperature, or buffer composition, pH, presence of glycerol or a detergent, etc.); water molecule coordinated to the heme iron (which keeps MTCYP51 in the low-spin state instead of the high-/low-spin state equilibrium in the absence of the substrate) can be seen in the structure of ligand-free MTCYP51 [1h5z] [41].

SDS -PAGE of the MTCYP51 mutants in the absence of β-mercaptoethanol (Fig 1B) shows that mutation C37L/C442A (lane 2) decreases the propensity of the protein to form disulfide bridges and suggests that the aditional C151A substitution (lane 3) is unnecessary. Lanes 4 and 5 demonstrate sharp increase in the intermolecular S-S bond formation upon mutation P187C, which confirms high surface exposure of the new C187 in the solution. Based on these data and taking into account significantly lower activity and the percentage of low-to-high spin transition in response to substrate with the mutant A197G/C37L/C151A/C442A/P187C (Table 1), we have chosen the A197G/C37L/C442A/P187C construct for selective chemical modification.

A197G/C37L/C442A/P187C-BODIPY

Modification of A197G/C37L/C442A/P187C with 3-fold molar excess of BODIPY-FL N-(2-aminoethyl)maleimide is complete within 10 min, the degree of labeling not exceeding 1.0 (M/M). Precipitation of the protein with acidic acetone confirmed absence of non-covalently bound dye (Figure 2A). The mutant A197G/C37L/C442A was not labeled at the same conditions, indicating that no residues other than C187 are accessible for modification with the thiol reactive probes; gel-filtration on Superdex 200 HR confirmed absence of the apoprotein aggregation.

In the absence of the heme fluorescence acceptor, BODIPY emission increases 6-fold (Figure 2B), which corresponds to the efficiency of FRET in the BODIPY/heme pair (Figure 2C) equal to 0.832 (from equation 3). Based on this value and in accordance with equation (2) the Förster radius [25] for the donor acceptor pair was calculated to be 41.7 Å. Using PhotochemCAD software as an automatic alternative for the calculations (refractive index

1.4, orientation factor 0.667, quantum yield 0.56, β-band absorbance maximum 536 nm (ε= 11.0 $mM^{-1}cm^{-1}$), wavelength range 450–550 nm) we obtained the same value. Overlapping emission and absorbance spectra of BODIPY and P450, respectively, and the calculated numbers are available as Supplementary Material, Figure 1.

Incorporation of the bulky fluorescent probe into the FG loop region of MTCYP51 causes about a 2-fold decrease in the enzymatic activity and a 1.6-fold decrease in maximal percentage of the protein which experiences low-to-high spin transition in the solution upon substrate addition. The ability to interact with azole inhibitors (ketoconazole and fluconazole were tested) was practically unchanged, the calculated apparent dissociation constants being 6.2±0.4 and 8.3±0.9 μM, respectively, (5.6±0.6 and 9.2±0.5 μM in the wild type MTCYP51), complete spectral transition to 424 nm Soret band maximum being achieved in both cases. Interaction with a non-metabolized sterol substrate analog estriol [41] was also not influenced by labeling, however, in the case of this ligand the percentage of maximal low-to-high spin transition was noticeably affected by mutation A197G (Kd ~30 μM, maximal high-spin form content 64% in the wild type MTCYP51 and only 45% in the A197G mutant).

FRET upon substrate and ligand binding, reduction and denaturation

In accordance with the fact that BODIPY incorporation into the FG loop of MTCYP51 did not influence binding of ketoconazole, fluconazole or estriol, addition of these ligands did not change BODIPY emission (not shown). Titration with lanosterol, however, results in gradual decrease in the fluorescence intensity (Figure 3). One additional CYP51 substrate, obtusifoliol, was tested and also found to cause comparable decrease in the BODYPY emission (not shown). Maximal achievable BODIPY quenching which corresponds to 22% of lanosterol bound MTCYP51 in the solution was 2.1-fold. In order to make further calculations, the observed linear dependence between decrease in BODIPY emission and portion of the substrate bound MTCYP51 was approximated to 100% high-spin P450 (Figure 3C), giving the value $F_{0\%}/F_{100\%} = 5.5$, which corresponds to the efficiency of FRET, equal to 0.97 (equation 3). Using the value of 41.7 Å as the Förster radius, in modified equation (1):

$$r^6 = R_0^6 \times (1/E - 1)$$

or PhotochemCAD produces 22.30 Å as the distance between BODIPY and the heme in the MTCYP51-lanosterol complex, which corresponds to an ~10 Å decrease in comparison with the distance in the ligand free structure (Figure 4). The value might not be precise because the calculations do not count possible differences between the distance in the structure and in solution or BODIPY orientation/dynamics including possible closer contact with one of the adjusted Tyr residues (Y181 or Y185) which might cause photoinduced electron transfer [42], but in principle the data prove that significant movement in the FG segment toward the heme, predicted by our previous work on MTCYP51 mutagenesis [23], does take place upon enzyme-substrate complex formation.

Opposite to the substrate binding, reduction of MTCYP51 with $Na_2S_2O_4$ followed by further conversion into the P420 form typical for this P450, causes increase in the intensity of BODIPY emission (1.4 and 2.0-fold, respectively). Increase in the active site volume may explain extreme destabilization of MTCYP51 upon reduction and is not surprising for protein denaturation.

Discussion

Conformational changes, from alterations in the orientation of single amino acid residues to segmental movements and rearrangements in secondary structural elements, appear to be a general feature of enzymatic mechanisms [43]. Based on information from the known crystal structures, in the CYP superfamily the range of motions available to a particular P450 seem to be connected with the breadth of its substrate specificity. Thus, using computational solvent mapping, it was hypothesized that while bacterial P450s have preformed substrate binding pockets, binding sites of drug-metabolizing mammalian P450s are formed in the process of interaction with substrate to adjust the shape and polarity necessary to accommodate different structures [12]. MTCYP51 is a representative of a CYP family which preserves very narrow substrate specificity [39]. No compounds other than five closely related natural sterols are metabolized. FRET- detected motion in the MTCYP51 FG segment suggests that large-scale conformational changes might be functionally important throughout this family having narrow substrate specificity. Restricting the configuration of the substrate in a position optimal for catalysis, such conformational changes might also be essential as a signaling tool from the protein matrix to the heme (e.g. changing the redox potential and the ability of the iron to bind oxygen [44]).

Showing that the MTCYP51 FG region is not involved in the interaction with estriol, the FRET data are in good agreement with structural information. Since estriol is much smaller and less hydrophobic than the CYP51 sterol substrates, the calculated apparent dissociation constant for the estriol-MTCYP51 complex is ~30-fold higher than for lanosterol. Apparently, binding of this ligand in the solution does not require additional rearrangements in the MTCYP51 substrate binding cavity. As for the azole derivatives tested, there are also no alterations in the FG-loop location in the fluconazole and 4-phenylimidazole-bound MTCYP51 crystals. On the other hand, these azoles are not strong MTCYP51 inhibitors, IC_{50}/P450 (M/M) being only of ~9, and 5 for fluconazole and ketoconazole, respectively. Taking into consideration that changes in the P450 structure might be dependent on the identity of the inhibitor bound [45] it is not excluded that conformational rearrangement, detectable by FRET analysis, might follow binding of more potent CYP51 inhibitors.

Until recently MTCYP51 was the only P450 in which the BC loop (at least upon crystallization) acquires an open conformation. Because accessibility of the heme to the solvent is not typical for cytochromes P450 (it has now also been observed in CYP8A1 (PGIS) [46]) it is very likely that the opening closes when substrate enters the active site [14]. Our attempts to study this region, however, were unsuccessful, because site-directed mutagenesis of MTCYP51 BC-loop residues was found to strongly affect functional characteristics or abolish P450 expression.

MTCYP51 is a unique P450 because it is a soluble protein that catalyzes the same reaction as do membrane bound forms of CYP51. Consequently determination of the MTCYP51 high resolution structure by X-ray crystallography has been very important in providing insight into the structure of the many membrane bound forms of the CYP51 gene family. However, because of the very nonpolar nature of CYP51 substrates it has not been possible to co-crystallize MTCYP51 with bound substrate. Using FRET analysis as described herein we have demonstrated that significant conformational movement occurs in the FG-segment approaching it closer to the heme group, the type of movement observed in many other forms of cytochrome P450 upon ligand binding. However, since it has not been found possible to use FRET to examine changes in the BC region of MTCYP51, our understanding of conformational changes that take place upon substrate binding to CYP51 remains incomplete and emphasizes the need to generate crystals of the substrate bound CYP51 complex.

Supplementary Material

Refer to Web version on PubMed Central for supplementary material.

Acknowledgments

The authors congratulate their colleague Fred Guengerich for his many contributions to P450 research around the world and at Vanderbilt. This work was supported by the National Institutes of Health grants GM067871 and ES 00267-32 (WRW), GM0030910-23 award to Dr. Richard Armstrong which supports NVS, the Slovenian Research Agency grants J1-6713 and the bilateral grant BI-US/06-07/019. MS is supported by the postgraduate fellowship from the Slovenian Research Agency.

References

1. Orengo CA, Michie AD, Jones S, Jones DT, Swindells MB, Thornton JM. Structure 1997;5:1093–108. [PubMed: 9309224]
2. Poulos TL. Proc Natl Acad Sci U S A 2003;100:13121–13122. [PubMed: 14597705]
3. Li H, Poulos TL. Curr Top Med Chem 2004;4:1789–802. [PubMed: 15579108]
4. Dunn AR, Dmochowski IJ, Bilwes AM, Gray HB, Crane BR. Proc Natl Acad Sci U S A 2001;98:12420–12425. [PubMed: 11606730]
5. Park SY, Yamane K, Adachi S, Shiro Y, Maves SA, Weiss KE, Sligar SG. J Inorg Biochem 2002;91:491–501. [PubMed: 12237217]
6. Zhao B, Waterman MR, Isin EM, Sundaramoorthy M, Podust LM. Biochemistry 2006;45:7493–7500. [PubMed: 16768445]
7. Scott EE, White MA, He YA, Johnson EF, Stout CD, Halpert JR. J Biol Chem 2004;279:27294–27301. [PubMed: 15100217]
8. Wester MR, Johnson EF, Marques-Soares C, Dijols S, Dansette PM, Mansuy D, Stout CD. Biochemistry 2003;42:9335–9345. [PubMed: 12899620]
9. Wester MR, Yano JK, Schoch GA, Yang C, Griffin KJ, Stout CD, Johnson EF. J Biol Chem 2004;279:35630–35637. [PubMed: 15181000]
10. Pylypenko O, Schlichting I. Annu Rev Biochem 2004;73:991–1018. [PubMed: 15189165]
11. Otyepka M, Skopalik J, Anzenbacherova E, Anzenbacher P. Biochim Biophys Acta 2007;1770:376–389. [PubMed: 17069978]
12. Clodfelter KH, Waxman DJ, Vajda S. Biochemistry 2006;45:9393–9407. [PubMed: 16878974]
13. Lepesheva GI, Zaitseva NG, Nes WD, Zhou W, Arase M, Liu J, Hill GC, Waterman MR. J Biol Chem 2006;281:3577–3585. [PubMed: 16321980]
14. Podust LM, Poulos TL, Waterman MR. Proc Natl Acad Sci USA 2001;98:3068–3073. [PubMed: 11248033]
15. Meharenna YT, Li H, Hawkes DB, Pearson AG, De Voss J, Poulos TL. Biochemistry 2004;43:9487–9494. [PubMed: 15260491]
16. Wester MR, Johnson EF, Marques-Soares C, Dansette PM, Mansuy D, Stout CD. Biochemistry 2003;42:6370–6379. [PubMed: 12767218]
17. Williams PA, Cosme J, Ward A, Angove HC, Matak Vinkovic D, Jhoti H. Nature 2003;424:464–468. [PubMed: 12861225]
18. Schoch GA, Yano JK, Wester MR, Griffin KJ, Stout CD, Johnson EF. J Biol Chem 2004;279:9497–94503. [PubMed: 14676196]
19. Williams PA, Cosme J, Vinkovic DM, Ward A, Angove HC, Day PJ, Vonrhein C, Tickle IJ, Jhoti H. Science 2004;305:683–686. [PubMed: 15256616]
20. Yano JK, Wester MR, Schoch GA, Griffin KJ, Stout CD, Johnson EF. J Biol Chem 2004;279:38091–38094. [PubMed: 15258162]
21. Gotoh O. J Biol Chem 1992;267:83–90. [PubMed: 1730627]
22. Podust LM, Stojan J, Poulos TL, Waterman MR. J Inorg Biochem 2001;87:227–235. [PubMed: 11744060]
23. Lepesheva GI, Virus C, Waterman MR. Biochemistry 2003;42:9091–9101. [PubMed: 12885242]

24. Zhao Y, White MA, Muralidhara BK, Sun L, Halpert JR, Stout CD. J Biol Chem 2006;281:5973–5981. [PubMed: 16373351]
25. Lakowicz, JR. Principles of Fluorescence Spectroscopy. Plenum Press; New York: p. I983
26. Anderluh G, Hong Q, Boetzel R, MacDonald C, Moore GR, Virden R, Lakey JH. J Biol Chem 2003;278:21860–21868. [PubMed: 12679333]
27. Croney JC, Cunningham KM, Collier RJ, Jameson DM. FEBS Lett 2003;550:175–178. [PubMed: 12935906]
28. Xiao M, Reifenberger JC, Wells AL, Baldacchino C, Chen LQ, Ge P, Sweeney HL, Selvin PR. Nat Struct Biol 2003;10:402–408. [PubMed: 12679807]
29. Smirnova IN, Kasho VN, Kaback HR. Biochemistry 2006;45:15279–15287. [PubMed: 17176050]
30. Kajihara D, Abe R, Iijima I, Komiyama C, Sisido M, Hohsaka T. Nature Methods 2006;3:923–929. [PubMed: 17060916]
31. Selvin PR. Nat Struct Biol 2006;9:730–7304.
32. Heyduk T. Curr Opin Biotechnol 2002;4:292–296. [PubMed: 12323348]
33. Corry B, Rigby P, Liu ZW, Martinac B. Biophys J 2005;89:L49–51. [PubMed: 16199508]
34. Bernhardt R, Dao NTN, Stiel H, Ruckpaul K. Biochim Biophys Acta 1983;745:140–148. [PubMed: 6405789]
35. Lepesheva GI, Strushkevich NV, Usanov SA. Biochim Biophys Acta 1999;1434:31–43. [PubMed: 10556557]
36. Davydov DR, Botchkareva AE, Davydova NE, Halpert JR. Biophys J 2005;89:418–432. [PubMed: 15834000]
37. Tsalkova TN, Davydova NY, Halpert JR, Davydov DR. Biochemistry 2007;46:106–119. [PubMed: 17198380]
38. Lepesheva GI, Podust LM, Bellamine A, Waterman MR. J Biol Chem 2001;276:28413–28284. [PubMed: 11373285]
39. Lepesheva GI, Waterman MR. Biochim Biophys Acta 2007;1770:467–477. [PubMed: 16963187]
40. Lepesheva GI, Zhou W, Nes WD, Waterman MR. Biochemistry 2004;43:10789–17899. [PubMed: 15311940]
41. Podust LM, Yermalitskaya LV, Lepesheva GI, Podust VN, Dalmasso EA, Waterman MR. Structure 2004;11:1937–1945. [PubMed: 15530358]
42. Marme N, Knemeyer JP, Sauer M, Wolfrum J. Bioconjug Chem 2003;6:1133–1139. [PubMed: 14624626]
43. Hammes GC. Biochemistry 2002;41:8221–8228. [PubMed: 12081470]
44. Hudecek J, Hodek P, Anzenbacherova E, Anzenbacher P. Biochim Biophys Acta 2007;1770:413–419. [PubMed: 17123739]
45. Yano JK, Koo LS, Schuller JS, Li H, Ortiz de Monetellano PR, Poulos TL. J Biol Chem 2000;275:31086–31092. [PubMed: 10859321]
46. Chiang CW, Yeh HC, Wang LH, Chan NL. J Mol Biol 2006;364:266–274. [PubMed: 17020766]

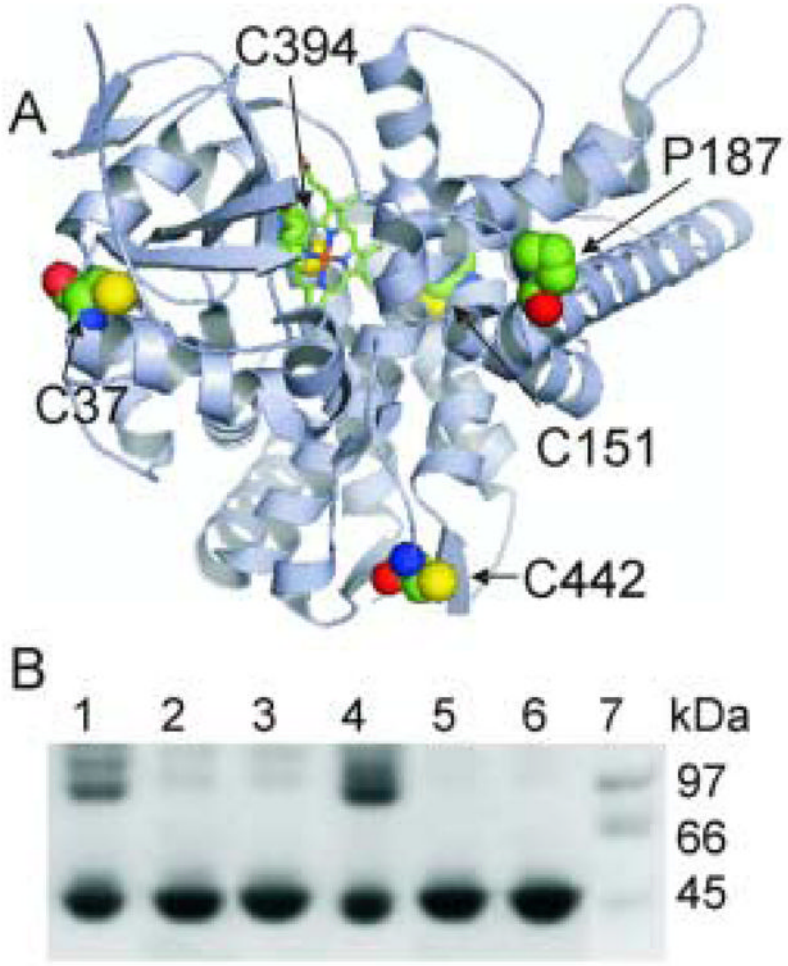

Figure 1.
MTCYP51 mutagenesis. A. Location of P187 and internal cysteine residues in the MTCYP51 structure (distal view). Surface accessibilities: P187~65%, C37~16%, C151~7%, C442~18%. Cys 394 is coordinated to the heme iron and can not be modified (prepared in PyMOL). B. SDS -PAGE of MTCYP51 mutants in the absence of β-mercaptoethanol. Lane 1, A197G; lane 2, A197G/C37L/C151A/C446A; lane 3, A197G/C37L/C446A; lane 4, A197G/C37L/C446A/P187C; lane 5, A197G/C37L/C446A/P187C DTT reduced (1:200); lane 6, A197G/C37L/C446A/P187C-BODIPY; lane 7, rainbow marker.

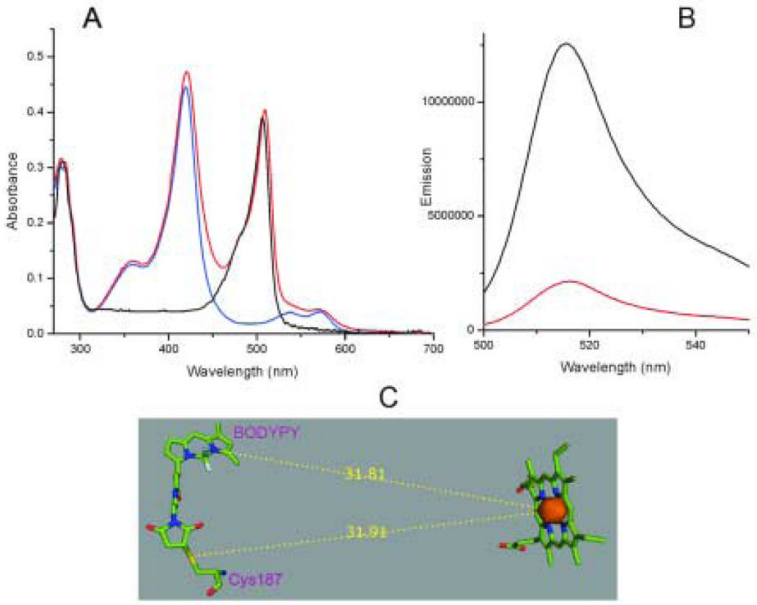

Figure 2.

MTCYP51 (A197G/C37L/C442A/P187C) – BODIPY, holo- (red line), apo- (black line); and unlabeled (blue line) protein. A. Absorbance spectra. The practically equal absorption at 280 nm in all three samples indicates that no significant changes occur in the structure of the protein globule upon heme removal. B. fluorescence spectra,. C. BODIPY modeled into the MTCYP51 structure [1H5Z] where P187 is mutated to C. In all calculations the assumption was made that the distance between the fluorophor and the heme in the solution corresponds to the distance between Cys187 and heme in the structure (31.97Å, as in Fig 4. In the model the distance is 31.91 as a result of energy minimization).

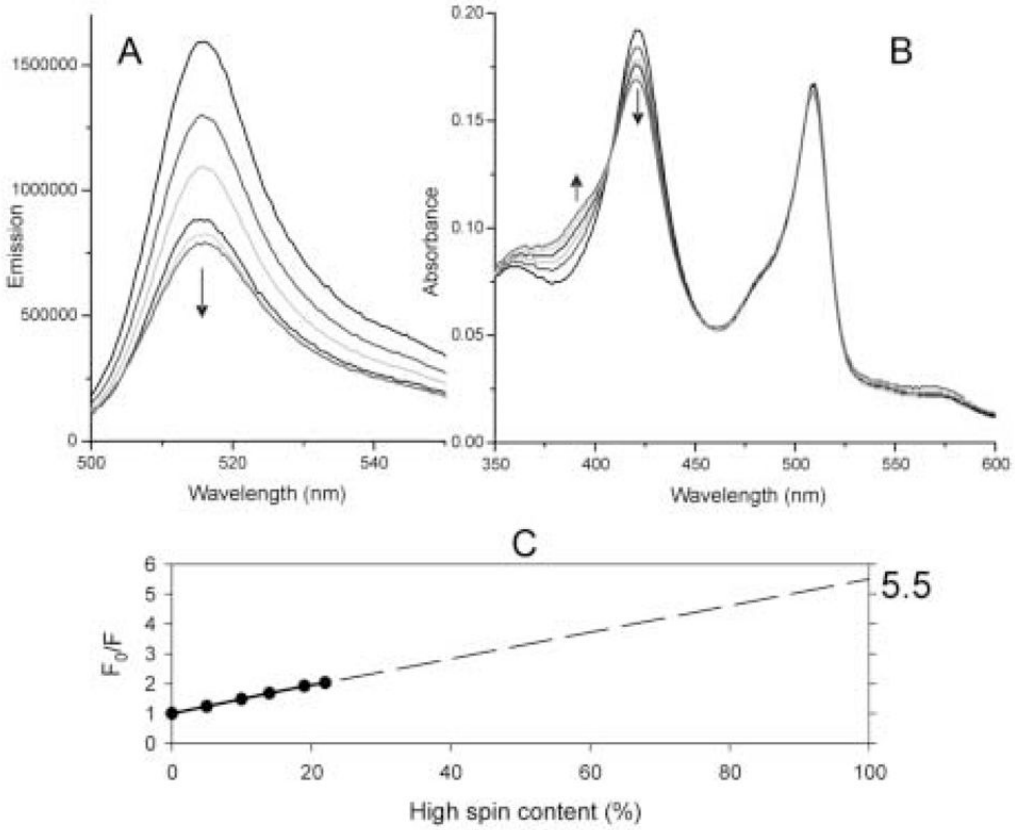

Figure 3.

Changes upon titration with lanosterol (0.5, 1.5, 2.5, 3.5 and 4.5 μM). A. BODIPY emission. B. Soret band absorbance. Arrows show the directions of changes. A very similar pattern was observed upon titration of 6-IAF-labelled MTCYP51 with lanosterol (not shown) C. Correlation between decrease in BODIPY emission and high-spin content in the MTCYP51 sample. Because the dependence is linear up to the maximal reachable high-spin content for the MTCYP51 A197G/C37L/C442A/P187C-BODIPY (22%, Table 1), to be able to calculate total changes we approximated fluorescence changes to the 100% high-spin P450.

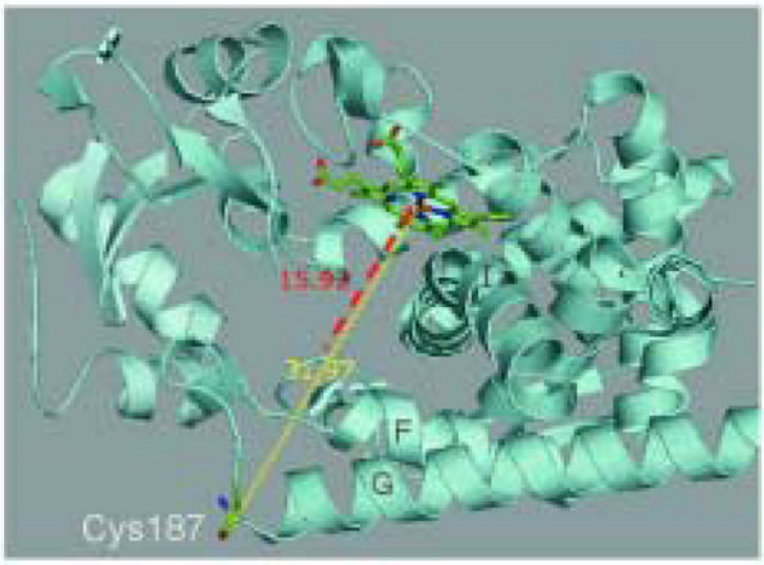

Figure 4.
Conformational changes in the FG segment of MTCYP51 calculated using FRET. Upper view of the structure (residues 77–90 of the BC-loop are omitted). Red dotted line shows the calculated distance between the heme and Cys187 in lanosterol bound MTCYP51.

Table 1

MTCYP51 construct for selective chemical modification with fluorophor

Mutation	Expression, %WT*	Activity, %WT	Spectral response to lanosterol, %WT (max high-spin)*
C37L	87	145	102 (18)
C151A/G/T	11/5/nd	82/nd/−	51 (9)
C442A/G	65/39	100/89	83 (15)
P187C	71	55	79 (14)
A197G	108	830	394 (71)
A197/P187C	51	460	200 (36)
A197G/C37L/C151A/C442A/P187C	6	114	47 (7)
A197G/C37L/C442A/P187C	50	400	194 (35)
A197G/C37L/C442A/P187C-BODIPY	-	236	122 (22)

*the values were calculated for 1.5 μM MTCYP51 (absolute absorbance ε_{417}=117 mM^{-1} cm^{-1}). Decrease of the protein concentration increases maximal high-spin content but also increases the measurement errors, while at the concentration of about 10 μM spectral response does not exceed 5 %. Complete saturation of MTCYP51 with lanosterol is not reachable most likely because of its extremely poor solubility.